URANIUM-SERIES DATING OF TEPHRA-BANDED ALLAN HILLS ICE

Edward L. Fireman

Smithsonian Astrophysical Observatory, Cambridge, Massachusetts 02138, U.S.A.

Abstract: Tephra-banded ice samples from the main Allan Hills icefield, Antarctica, are dated by a uranium-series method, which is based on the $^{226}Ra/^{230}Th$ and $^{226}Ra/^{234}U$ ratios dissolved in ice from tephra. The consistence between the age determined from the $^{226}Ra/^{230}Th$ ratio with the age determined from the $^{226}Ra/^{234}U$ ratio serves as a check on the method. For ice from a location at the western border of the 50-km^2 area that is richly laden with meteorites, the $^{226}Ra/^{230}Th$ and $^{226}Ra/^{234}U$ ages are $(95\pm10)\times10^3$ and $(100\pm10)\times10^3$ years, respectively. For ice from a location within this meteorite-rich area near its eastern border (approximately 5 km closer to the Allan Hills land barrier), these ages are $(185\pm25)\times10^3$ and $(210\pm30)\times10^3$ years, respectively. The ice flow is from west to east, the dates indicate that most of the ice in the meteorite-rich area is between 1×10^5 and 2×10^5 years old with the age of the ice increasing in the flow direction as theoretically predicted for ice approaching a land barrier. The comparison of this ice chronology with the terrestrial ages of the meteorites leads to a number of conclusions about the meteorite fall rate and history of the ice movement.

1. Introduction

The Antarctic ice sheet preserves a long, continuous record of climatic conditions, volcanic activity, atmospheric contaminants, and meteorite infall. The dating of horizons within the ice is a prerequisite for constructing meaningful records based on correlations between different sites. A 150×10^3 year chronology was obtained from the 2083-m-deep core at Vostok by LORIUS *et al.* (1985) by associating variations of $^{18}O/^{16}O$ and $^2H/H$ ratios of the ice with flow calculations and the time of the Wisconsin glaciation. Ice cores are essential to many kinds of studies, but their small diameters, of 7 to 15 cm, and the difficulty of recovering deep cores samples limits their usefulness. We report here on dates obtained, by the uranium-series method, on blocks of near-surface ice collected from the main Allan Hills icefield, an expanse of ablating ice that serves as a meteorite stranding surface.

Ablation surfaces form where the shoreward flow of ice is inhibited by a mountain barrier. A continued push from inland ice forces the ice to flow upward by a mountain obstruction to the surface where the ice is abraded by wind. Many ablation areas exist in the Antarctic ice sheet because of the frequency of mountains. Exposed meteorites have been found on some of these ablation areas but not on others. A rectangularly shaped ice ablation area, approximately 10 km by 5 km, which has yielded more than 1000 meteorite specimens, borders the western flank of the Allan Hills at about 76°45′S; 159°E (CASSIDY, 1979; WHILLANS and CASSIDY, 1983). Bands

of dust have been observed in all ablating ice fields whether or not meteorites are present.   Keys *et al.* (1977) described tephra and debris layers in the Skelton Neve and the Kempe Glacier (South Victoria Land).   Most layers studied by Keys *et al.* (1977) were very dark brown to black, with high concentrations of material and a steep angle of dip.   They report most bands to consist of basanite tephra.   Nishio *et al.* (1985), Katsushima *et al.* (1984), and Fukuoka *et al.* (1985) investigated the composition and origin of dust bands in the Yamato Mountain area and the Allan Hills area; they found that volcanic debris makes up the bulk of the material.   Down-stream of the ablation area, the dust bands trend predominantly at an angle of about 90° to the direction of the ice flow; upstream of the ablation area, the bands are approximately parallel to the ice flow.   The bands are usually 10 to 25 cm wide at the surface but are narrower at depth.   In our samples of Allan Hills ice, taken from depths of 50 to 100 cm, the bands are 3 to 6 cm wide.   The ice samples have a high concentration of gas bubbles, similar to those found in deep ice cores.   Bubbles in the dusty bands are comparable in size and frequency to those in the clean ice.

Marvin (1986) investigated the dust bands in our ice samples and found that the particulates in the dust bands consisted mainly of volcanic glass shards with some associated mineral grains.   We assume that dust from individual eruptions was deposited on the surface of the snow, buried, and compressed into ice that, eventually,
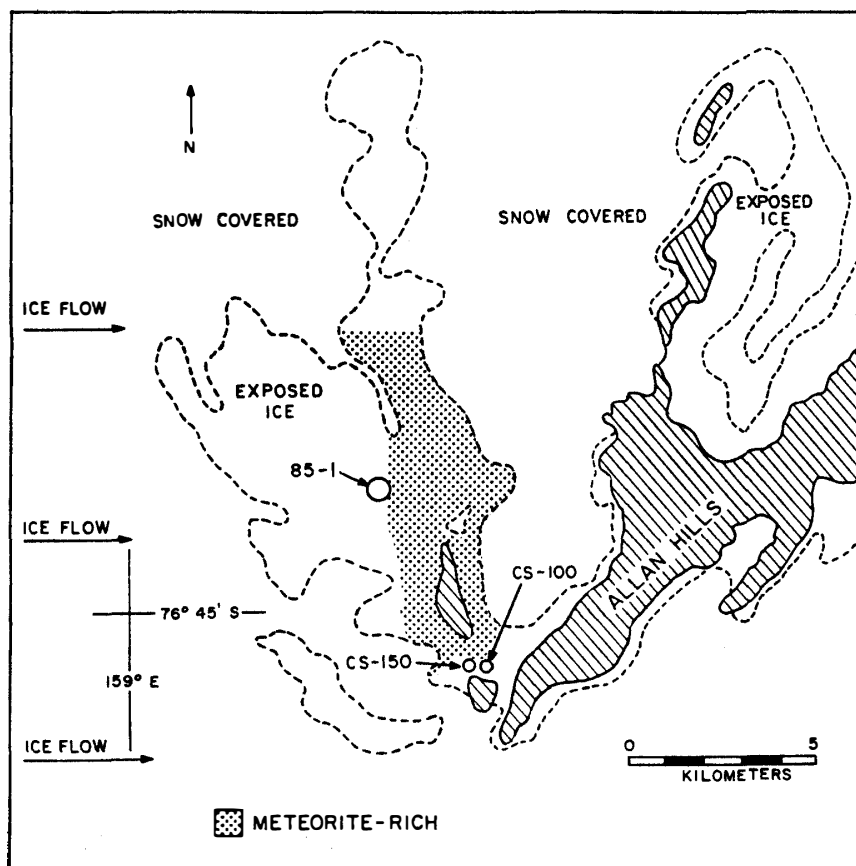

Fig. 1.   Map of main Allan Hills icefield showing the locations of the dated ice samples and the meteorite-rich area.

surfaced at the Allan Hills ablation site. Figure 1 is a map of the main Allan Hills icefield showing the locations of the tephra-banded ice samples, which we have dated. The sample labeled 85-1 is at the center of the western border of the 50-km² meteorite-rich area. The sample labeled CS-150 is near the eastern and southern borders of the meteorite-rich area just outside a cove containing very stagnant ice, called Cul de Sac. The sample labeled CS-100 is within this cove and close to the edge of a protruding land mass.

FIREMAN (1986a, b) obtained uranium-series ages of approximately 2×10^5 and 3×10^5 years for two dust-banded ice samples labeled CS-150 and CS-100; however, those determinations lacked uranium and thorium measurements on the embedded particulates. We have obtained those values and increased the reliability of the dates reported here. We also report uranium-series dates for the sample labeled, 85-1. The labels are field designations, which were on slips of paper enclosed in the plastic bags with the ice samples shipped to our laboratory.

2. Experimental Procedure and Results

The ice samples are melted and filtered with the temperature of the melt water at approximately 0°C and its pH approximately 1.0. The ^{226}Ra, ^{230}Th, ^{234}U, and ^{238}U activities in the filtered water are then determined by the analytical procedures that have been described (FIREMAN, 1986a). Table 1 gives the masses of the ice aliquots analyzed from the larger blocks that were received, the visual appearance of the ice aliquot, the dust content of the ice aliquot, and the activities measured. Two samples were removed from each block. One sample, containing the center of the band,

Table 1. Uranium-series nuclide activities dissolved in the ice and in the dust particles.

Field designation	CS-100	CS-150	85-1
Ice aliquot	1.00 kg	1.87 kg	1.63 kg
Visual appearance	heavy band	light band	medium band
Dust (g)/ice (kg)	0.30	0.070	0.210
^{226}Ra (filtered H_2O)*	0.198±0.007	0.109±0.004	0.144±0.004
^{230}Th (filtered H_2O)*	0.130±0.005	0.070±0.001	0.080±0.001
^{234}U (filtered H_2O)*	0.062±0.003	0.042±0.001	0.049±0.001
^{238}U (filtered H_2O)*	0.006±0.003	0.020±0.001	0.031±0.001
Ice aliquot	0.90 kg	3.69 kg	1.40 kg
Visual appearance	band edge	clear	clear
Dust (g)/ice (kg)	0.15	0.007	0.002
^{226}Ra (filtered H_2O)*	0.109±0.007	0.023±0.002	0.014±0.002
^{230}Th (filtered H_2O)*	0.080±0.006	0.022±0.001	0.013±0.002
^{234}U (filtered H_2O)*	0.043±0.003	0.020±0.001	0.014±0.001
^{238}U (filtered H_2O)*	0.009±0.003	0.020±0.001	0.015±0.001
^{230}Th (dust†)*	1400±200	not measured	3700±200
^{234}U (dust†)*	1500±100	not measured	4100±200
^{238}U (dust†)*	1500±100	not measured	4100±200

* Activity values in dpm kg^{-1} units (decays per min per kg).
† 0.019 g aliquot of dust used for activity measurements.

was the dustiest available; the other contained either an edge of the band or was completely clear.

A 19-mg aliquot of the separated dust is used for the [230]Th, [234]U, and [238]U activity measurements. The results are given in the bottom three rows of Table 1. The experimental procedure used for these analyses follows. Approximately 20 ml of concentrated HCl with [232]U and [228]Th carriers and 1 ml of concentrated HF are added to 19 mg of particulates and the particulates completely dissolve. The solution is boiled down to 1 ml in a platinum crucible and taken up in 50 ml of distilled water and its pH is adjusted to 1.0 by adding NH_4OH. The uranium and thorium are solvent-extracted into an equal volume of 0.032 mol DEHP (diethylhexyl phosphoric acid) in toluene and back-extracted into 20 ml of concentrated HCl. The solvent extraction and back extractions are repeated three times. The 120 ml HCl of back extract is passed through a DOWEX-1 resin column. The thorium passes through the column with the HCl. The uranium is removed from the column with 120 ml of pH=0.85 water. The separated uranium and thorium solutions are evaporated to 1 ml and electro-deposited on stainless-steel disks, which are alpha-counted with surface barrier detectors and multi-channel analyzers.

For the dusty ice samples (0.070 to 0.30 g of dust per kg ice), the activities dissolved
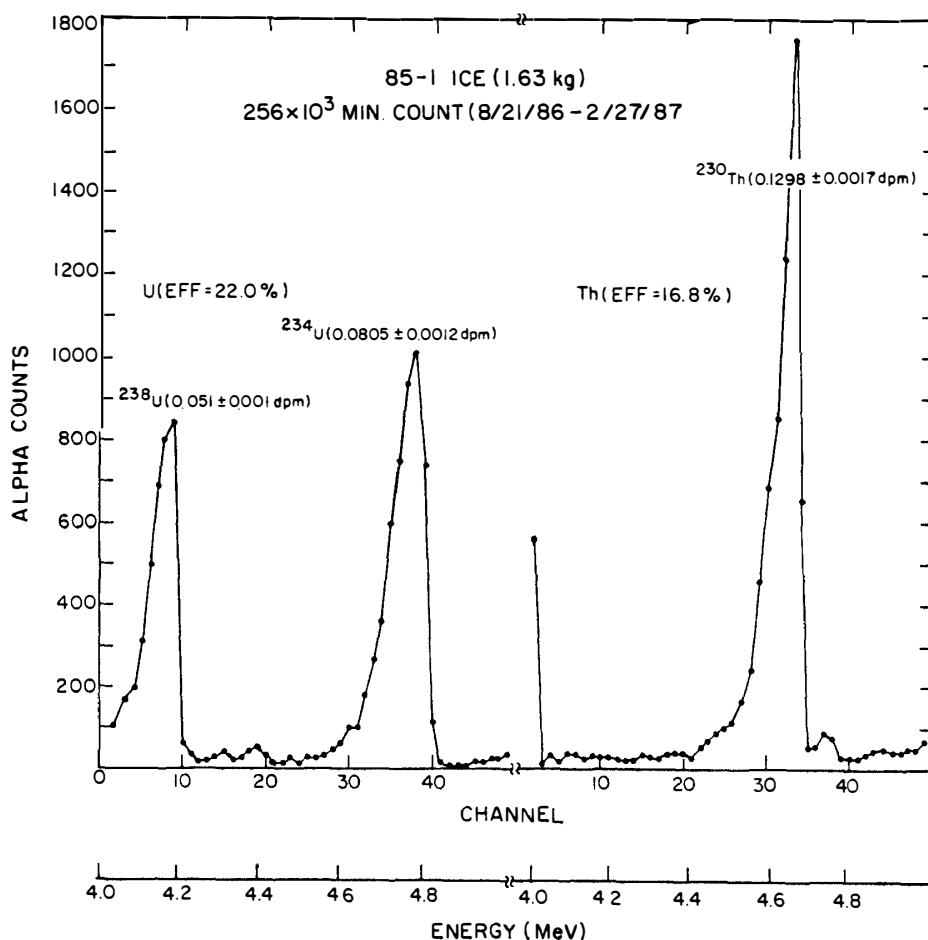

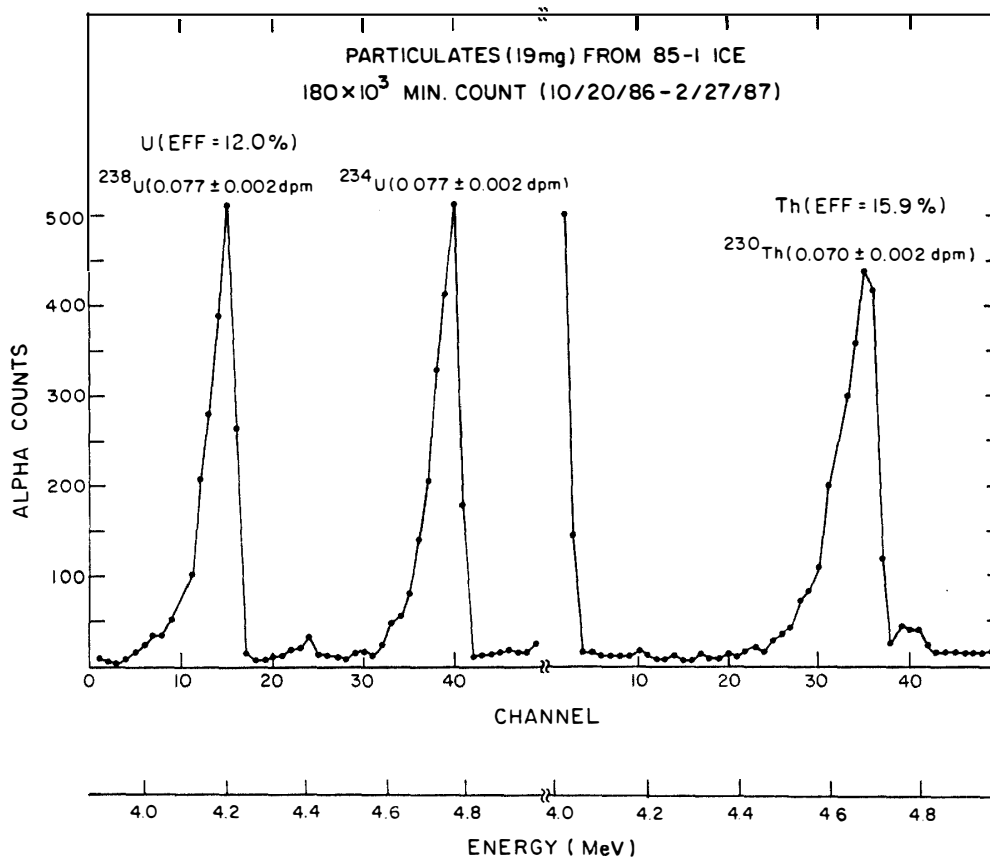Fig. 2.   Alpha count data for unraium-series nuclides dissolved in dusty ice sample, 85-1.

Fig. 3. *Alpha count data for particulates separated from dusty ice sample, 85-1.*

in the filtered water are disequilibrated. The ^{226}Ra activity is between 30% and 80% higher than that of its parent ^{230}Th, more than a factor of 2 higher than that of its grandparent ^{234}U, and more than a factor of 3 higher than that of its great grandparent ^{238}U. For the clear ice, the dissolved activities are in radioactive equilibrium. For the dust itself, activities are also in equilibrium. Figure 2 presents the alpha-count data for the nuclides dissolved in dusty ice sample, 85-1; Fig. 3 presents alpha-count data for a 19-mg aliquot of the particulates separated from this ice.

The uranium concentration in the particulates is approximately 10^5 times higher than in the ice. The transfer of a few percent of the daughters from the particulates to the ice would not be observable in the particulates but would be very noticeable in the ice. Transfer of daughters to the ice could arise from the recoils of alpha decay products out of the particulates or from the dissolution of particulate material. We consider both possibilities.

3. Interpretation of Data and the Ages

The alpha recoil mechanism was discussed by FIREMAN (1986a). This mechanism adds ^{226}Ra, ^{230}Th, and ^{234}U, but not ^{238}U to the ice from near-surface particulate material. The range of the ^{226}Ra, ^{230}Th, and ^{234}U products in glass is approximately 3×10^{-6} cm; therefore the particulates must be extremely fine or very irregular and
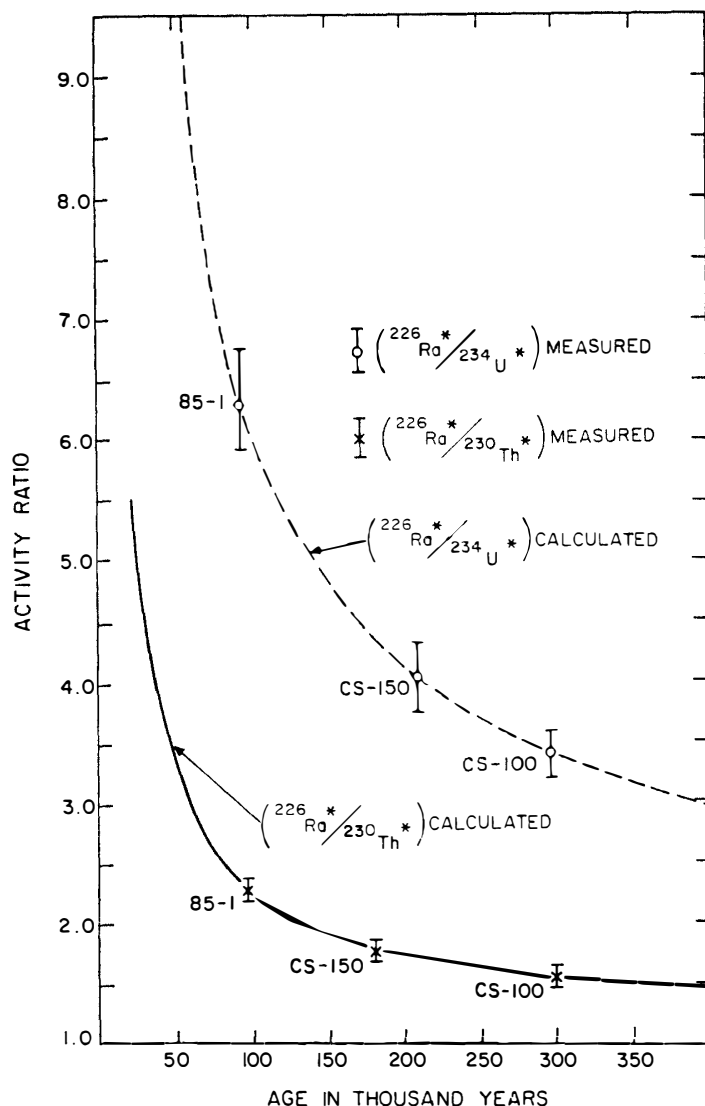
Fig. 4.   Ratios of activities (*added to ice from tephra*) *versus age.*

bubbly for a few percent of the recoils to go into the ice. Irregular shapes and vesicles are, in fact, observed in the glassy particulates. Although the magnitudes of the daughter additions depend upon the shapes and sizes of the particulates, the ^{226}Ra/ ^{230}Th or the ^{226}Ra/^{234}U ratios of the additions are independent of particulate shapes and sizes. These activity ratios change with time in a calculable manner shown by the solid and dashed curves in Fig. 4, which are obtained from FIREMAN's (1986a) calculation. The age on the abscissa of Fig. 4, is the time since the particulates became embedded in the ice.

The dissolution of particulate material (both unaltered material and material altered by contact with the ice) requires ice melting. On the basis of the high bubble content throughout the ice samples, we conclude that no prior melting has occurred. Melted refrozen polar ice has a distinctly different texture than that observed in our Allan Hills samples. Some dissolution of particulate material can occur during our melting and filtering procedure. If average particulate material is dissolved, the

nuclide contributions to the ice are in radioactive equilibrium and the recoil ages are not changes. If alpha-particle-damaged material on the surface of the particulates is preferentially dissolved, the ^{226}Ra/^{230}Th or the ^{226}Ra/^{234}U ratio in the dissolved material corresponds to the time since the damaging began. For volcanic glass shards, the alpha damaging began as soon as the glass cooled shortly after the eruption. The contents of ^{238}U dissolved in the CS-100 and CS-150 ice samples are very low and indicate that dissolution of particulate material did not occur. For the 85-1 ice samples, the ^{238}U content is higher in the dusty than in the clear sample, indicating that some particulate material dissolved. The 85-1 volcanic material, preferentially dissolved from alpha-particle-damaged surface sites, contains ^{234}U, ^{230}Th, and ^{226}Ra excesses that are determined by the age of the volcanic material. If the material dissolution occurred during the laboratory melting and filtering, then the uranium series age would not be noticeably affected, because the ages of the volcanics and the imbedding ice are essentially the same. If the dissolution of this material occurred at an earlier time, then the measured uranium-series age would be younger than the age of the ice. Because the dusty ice has the same gas bubble content as the neighboring clear ice, both the dusty and clear ice were formed from snow and the ice has remained solid since its formation. We consider the dissolution of particulate material into solid ice to be unlikely; therefore, we consider it to be unlikely that the uranium-series age of the 85-1 ice sample is reduced by prior dissolution of particulate material.

Table 2 gives the excess ^{226}Ra, ^{230}Th, and ^{234}U activities dissolved in the ice (i.e., the activity of the nuclide minus that of ^{238}U), the ratios of the excess activities, and the ages that result from these ratios.

The 85-1 sample has the youngest age, $(100\pm10)\times10^3$ years from the ^{226}Ra/^{230}Th ratio and $(95\pm10)\times10^3$ years from the ^{226}Ra/^{234}U ratio. The CS-150 ice has ages of $(180\pm25)\times10^3$ years and $(210\pm30)\times10^3$ years; the larger errors are due to the fact that the activity ratios change more slowly as the age increases. The dustier CS-100 sample has ages of $(300^{+100}_{-80})\times10^3$ and $(290^{+70}_{-50})\times10^3$ years. The consistency of the

Teble 2. Excess activities* (dissolved) and uranium-series ages.

	CS-100 (1.00 kg)	CS-150 (1.87 kg)	85-1 (1.63 kg)
^{226}Ra* (dpm kg^{-1})	0.192±0.007	0.089±0.004	0.113±0.004
^{230}Th* (dpm kg^{-1})	0.124±0.006	0.050±0.0016	0.049±0.0014
^{234}U* (dpm kg^{-1})	0.056±0.004	0.022±0.0014	0.018±0.0014
^{226}Ra*/^{230}Th*	1.55±0.09	1.78±0.10	2.31±0.10
Age (years)	$(300^{+100}_{-80})\times10^3$	$(180\pm25)\times10^3$	$(100\pm10)\times10^3$
^{226}Ra*/^{234}U*	3.43±0.27	4.05±0.32	6.28±0.51
Age (years)	$(290^{+70}_{-50})\times10^3$	$(210\pm30)\times10^3$	$(95\pm10)\times10^3$
Ave. Age (years)	$(295^{+60}_{-40})\times10^3$	$(195\pm20)\times10^3$	$(98\pm7)\times10^3$

* Excess activity=activity minus the ^{238}U activity.
^{226}Ra (half life=1622 years)
^{230}Th (half life=75000 years)
^{234}U (half life=247000 years)

ages obtained from the two ratios is very good.

4. Comparison with the Meteorite Terrestrial Ages

Approximately a thousand meteorites have been recovered from an approximately 10 km × 5 km area of exposed ice west of the Allan Hills land barrier. Terrestrial ages (elapsed time since fall) have been measured for more than 80 meteorites from the main Allan Hills icefield. Some of these meteorites are paired. From the more than 80 specimens, we obtain 55 that appear to be independent falls. These consist of 5 meteorites with ^{14}C terrestrial ages less than 30000 years (determined by Fireman and co-workers) and 50 meteorites with ^{36}Cl terrestrial ages (determined by Nishiizumi and co-workers). The youngest is 11000 years (Fireman, 1980); the oldest is 950000 years (Nishiizumi et al., 1986). Approximately 20% of these meteorites are between 0 and 1×10^5 years old; 65% are between 1×10^5 and 4×10^5 years old; and 15% are between 4×10^5 and 10^6 years old. Meteorites less than 10^5 years must have fallen directly onto the older ice. Some of these (particularly the small specimens) could have been lost by wind transport and by weathering. Winds need to move meteorites only to a snow covered area for them to be hidden. According to field studies (W. A. Cassidy, private commun., 1988), meteorites less than 200 g are readily moved by wind; however, age determinations have been made only on specimens above that size. In the 50 km^2 area most richly laden with meteorites, there are 240 specimens heavier than 200 g; their average weight is 1.4 kg. The mass influx, averaged over the past 10^5 years is therefore estimated to have the lower limit value of $(0.20)(240)(1.4 \text{ kg})/(50 \text{ km}^2)(10^5 \text{ years})$ or $1.3 \times 10^{-5} \text{ kg km}^{-2} \text{ yr}^{-1}$. The Halliday et al. (1984) photographic results indicate that 8 meteorites (≥ 1 kg) fall in a 10^6 km^2 area per year. The agreement between 10^5 year average and the observed influx during recent times indicates that the fall rate has been approximately constant. The terrestrial age distribution is essentially flat between 0 and 4×10^5 years and has a dramatic decrease at 4×10^5 years so that the meteorites between 4×10^5 and 10^6 years old are underabundant relative to the constant fall expectation. None of the 80 dated meteorites are older than 10^6 years; their absence may be caused by weathering or by a change in the ice sheet thickness that caused the removal of the older meteorites. During the time period, 1×10^5 to 4×10^5 years, the meteorite accumulation rate by ice transport into the 50 km^2 area was essentially balanced by loss mechanisms (weathering and transport away). Ice transport and weathering rates depend upon the climate. It is tempting to associate the dramatic decrease in the terrestrial age distribution at 4×10^5 years with a very warm climate at that time; which caused most of the older meteorites to weather away.

References

CASSIDY, W. A. (1979): Antarctic meteorites. EOS; Trans. Am. Geophys. Union, 60, 175–177.

FIREMAN, E. L. (1980): Carbon-14 and argon-39 in ALHA meteorites. Proc. Lunar Planet. Sci. Conf., 11th, 1215–1221.

FIREMAN, E. L. (1986a): Uranium series dating of Allan Hills ice. J. Geophys. Res., 91, B4, D539–544.

FIREMAN, E. L. (1986b): Uranium series dating of Allan Hills ice. J. Geophys. Res., 91, B8, 8393.

FUKUOKA, T., ARAI, F. and NISHIO, F. (1985): Identification of tephra layers in the meteorite ice field based on trace element compositions and refractive indices of glass. Mem. Natl Inst. Polar Res., Spec. Issue, 39, 250.

HALLIDAY, I., BLACKWELL, A. T. and GRIFFIN, A. A. (1984): The frequency of meteorite falls on the earth. Science, 223, 1405–1407.

KATSUSHIMA, T., NISHIO, F., OHMAE, H., ISHIKAWA, M. and TAKAHASHI, S. (1984): Composition of dirt layers in the bare ice areas near the Yamato Mountains in Queen Maud Land and the Allan Hills in Victoria Land, Antarctica. Mem. Natl Inst. Polar Res., Spec. Issue, 34, 174–187.

KEYS, J. R., ANDERTON, P. W. and KYLE, P. R. (1977): Tephra and debris layers in the Skelton Neve and Kempe Glacier, South Victoria Land, Antarctica. N. Z. J. Geol. Geophys., 20, 971–1002.

LORIUS, C., JOUZEL, J., RITZ, C., MERLIVAT, L., BARKOV, N. J., KOROTKEVICH, Y. S. and KOTLYAKOV, V. M. (1985): A 150,000-year climate record from Antarctic ice. Nature, 316, 591–596.

MARVIN, U. B. (1986): Components of dust bands in ice from Cul de Sac, Allan Hills region, Antarctica. Meteoritics, 21, 442–443.

NISHIIZUMI, K., ELMORE, D., KUBIK, P. W., BONAMI, G., SUTER, M., WOLFI, W. and ARNOLD, J. R. (1986): Ages of Antarctic meteorites and ice. Lunar and Planetary Science XVII. Houston, Lunar Planet. Inst., 621–622.

NISHIO, F., KATSUSHIMA, T. and OHMAE, H. (1985): Volcanic ash layers in bare ice areas near the the Yamato Mountains, Dronning Maud Land and the Allan Hills, Victoria Land, Antarctica. Ann. Glaciol., 7, 34–41.

WHILLANS, I. M. and CASSIDY, W. A. (1983): Catch a falling star; Meteorites and old ice. Science, 222, 55–57.